

# Cisplatin-functionalized silica nanoparticles for cancer chemotherapy

Chandrababu Rejeeth · Tapas C. Nag ·  
Soundarapandian Kannan

Received: 27 May 2013 / Accepted: 1 July 2013 / Published online: 20 July 2013  
© Springer-Verlag Wien 2013

**Abstract** Cisplatin is used to treat a variety of tumors, but dose-limiting toxicities or intrinsic and acquired resistance limit its application in many types of cancer including breast. Cisplatin was attached to silica nanoparticles using aminopropyltriethoxy silane as a linker molecule and characterized in terms of size, shape, as well as the dissolution of cisplatin from the silica surface. The primary particle diameter of the as received silica nanoparticles ranged from 20 to 90 nm. The results show that adverse effects on cell function, as evidenced by reduced metabolic activity measured by the MTT assay and increased membrane permeability observed using the live/dead stain, can be correlated with surface area of the silica. Cisplatin-functionalized silica nanoparticles with the highest surface area incited the greatest response, which was almost equivalent to that induced by free cisplatin. Moreover, if verified by further studies, would indicate that cisplatin was attached to silica nanoparticles might prove to be useful in site-specific drug delivery.

**Keywords** Silica · Cisplatin · TEM · Nanoparticles · MCF-7 cells · Fluorescence

**Electronic supplementary material** The online version of this article (doi:10.1007/s12645-013-0043-6) contains supplementary material, which is available to authorized users.

C. Rejeeth (✉) · S. Kannan  
Proteomics and Molecular Cell Physiology Lab, Department of  
Zoology, School of Life Sciences, Bharathiar University,  
Coimbatore 641 046, TN, India  
e-mail: crejee@gmail.com

T. C. Nag  
Sophisticated Analytical Instrument Facility for Electron  
Microscopy, Department of Anatomy, All India Institute of Medical  
Sciences, New Delhi 110029, India

## 1 Introduction

Worldwide, deaths: an estimated 39,920 breast cancer deaths (39,510 women, 410 men) are expected in 2012. Breast cancer ranks second as a cause of cancer death in women (after lung cancer) (American Cancer Society 2012). Cis-diamminedichloroplatinum (II), known as cisplatin, a platinum-based drug, is one of the most potent antitumor agents has been widely used in the clinic to treat a variety of cancers such as ovarian, breast, bladder, head and neck, and small cell lung cancer because of its potent activity to cross-link DNA upon entering the cells (Wang and Lippard 2005). Chemotherapy is the mainstay treatment for advanced and metastatic disease. DNA-damaging agents have a long and proven record as anticancer drugs (Decatris et al. 2004). It is proved that after both passive and active cellular uptake, cisplatin may react with the N7 atom of guanine in DNA to form adducts and causes cellular apoptosis (Giese and McNaughton 2003). However, chronic cisplatin usage results in resistance by several possible mechanisms including increased interactions with metallothionein and glutathione as well as increased DNA repair (Reedijk 2003). To counteract resistance, which lowers the efficiency of cisplatin significantly, very high systemic doses of cisplatin are administered. Unfortunately, such high dose of cisplatin results in severe systemic toxicity and poor patient compliance, including nausea/vomiting, renal toxicity, gastrointestinal toxicity, peripheral neuropathy, asthenia, and ototoxicity, thus limiting its clinical use (Hill and Speer 1982; Rosenberg 1977). To improve the efficacy and safety of cisplatin, a variety of methods are applied to drug delivery system, which include particulate carriers, such as liposomes, polymers, and nanoparticles (NPs) (Bontha et al. 2006; Junior et al. 2007; Geng et al. 2004). The drug carriers may concentrate in the tumor because tumors exhibit a unique enhanced permeability and retention effect for 50–100 nm particles. As a result of this, a large increase in tumor drug

concentrations (tenfold or higher) could be achieved relative to administration of the same dose of free drug, (Maeda et al. 2000) thereby decreasing the massive systemic side effects of conventional chemotherapy. In our previous study on modified silica nanoparticles, (ORMOSIL, LSN) however, it was shown that the cytotoxicity across the MCF-7 cells as measured by methyl-thiazol tetrazolium salts (MTT) assay was significantly reduced for the case of silica nanoparticles synthesized and p53 gene delivery successful in breast cancer cell line (Rejeeth et al. 2012a; Rejeeth et al. 2012b). In the case of materials in combination, the relevant question is whether apparently non-toxic particles are transformed into a potentially toxic material if surface attached with known toxic molecules. Three possibilities exist: the nanoparticle/toxic molecule combination becomes more toxic, the toxicity of the combination is unchanged, or the toxicity of the combination is reduced compared to the toxic molecule alone. One common chemical used for surface functionalization is aminopropyltriethoxysilane (APTES), which has the chemical formula  $\text{NH}_2(\text{CH}_2)_3\text{-Si}(\text{OC}_2\text{H}_5)_3$  (Gan et al. 2009; Liu et al. 2009; Jang and Liu 2009; Libertino et al. 2008). The silane end of the APTES molecule binds covalently to surface silicon atoms, and the amino end of the molecule increases protein adsorption on the surface by electrostatic interactions. The structural transition of a single dsDNA molecule immobilized on an APTES-treated substrate has been demonstrated. DNA binding to the APTES linker is much stronger than that on an alkylthiol/substrate (Nguyen et al. 2009). Silica-cisplatin system provides a unique opportunity to explore effects of surface area, in terms of the ability of nanoparticles to serve as carriers. The testable hypothesis herein is that nontoxic nanoparticles with a surface-attached toxic molecule would then adversely affect cell function, defined here by reduced metabolic activity and increased membrane permeability. Specifically, these adverse effects are expected to increase with increasing surface area. Results of physicochemical characterization of the nanoparticles and nanoparticle/cisplatin combination including surface area and cisplatin dissolution rates are presented. Effects on metabolic activity as measured via the MTT assay, and membrane permeability observed by fluorescence microscopy using the DAPI/JC-1 live/dead stain, we demonstrated that these silica-cisplatin prodrug conjugate NPs had well-controlled drug loading yield, excellent acid-responsive drug release characteristics, and potent cytotoxicity against breast cancer.

## 2 Materials and methods

### 2.1 Materials

The chemicals, i.e., APTES (3-aminopropyl) triethoxysilane, Triton X-100, Cisplatin, DAPI and JC-1 (Sigma-Aldrich) were

used without further purification. All the glassware (glass bottle and small pieces of glass substrate) was cleaned and sonicated in ethanol for 5 min, rinsed with double-distilled water, soaked in a  $\text{H}_2\text{O}/\text{HNO}_3$  (65 %)/ $\text{H}_2\text{O}_2$  (1:1:1, v/v/v) solution, rinsed again with doubly distilled water, and finally dried in air. The MCF-7 cells were purchased from National Centre for Cell Sciences (NCCS), Pune, India.

### 2.2 Surface attachment of cisplatin to silica particles

Approximately, 0.64 g of APTES-functionalized Triton X-100, silica particles were kept in a three-necked flask respectively and dispersed in 50 mL distilled water with constant stirring for sample; 0.385 g of cisplatin was added for APTES-functionalized Triton X-100 samples of suspended silica particles, respectively. These amounts correspond to sufficient cisplatin to react with all available silanol groups ( $2.5 \text{ nm}^{-2}$ ) on the surface of silica. The suspended particles were constantly stirred under nitrogen over-night at room temperature inside the fume hood. Cisplatin-functionalized silica particles were then collected by centrifugation at 3,500 rpm for 15 min. Harvested particles were dried at room temperature and stored in glass bottles for further analysis.

### 2.3 FT-IR of cisplatin-functional silica nanoparticles

Fourier transform infrared (FT-IR) spectroscopy of silica nanoparticle, cisplatin, and cisplatin-functionalized silica nanoparticles were performed by using Nicolet 5700 instrument (Nicolet Instrument, Thermo Company, USA) with KBr pellet method. Each KBr disk was scanned over a wave number region of 500–4,000  $\text{cm}^{-1}$  with the resolution of  $4.0 \times 10^8 \text{ cm}^{-1}$ .

### 2.4 Cisplatin estimation

The platinum content of cisplatin-functionalized silica particles was measured by inductively coupled plasma-mass spectrometry (ICP-MS) measurements; 0.020 g of cisplatin functionalized silica particles was added to 25 mL of 2 %  $\text{HNO}_3$ . The suspension was sonicated in an ultrasonic bath for 30 min. After centrifugation, a clear supernatant was obtained which was analyzed for total platinum (Pt). The platinum content of the sample was determined by comparison with a platinum standard which was prepared by dilution of a standard solution of platinum of defined concentration. The total amount of platinum measured from the sample was converted into the amount of cisplatin.

### 2.5 Transmission electron microscopy

Particle morphology was observed using a field emission transmission electron microscope (TEM). The selected area

diffraction patterns of the samples were recorded using the same TEM instrument. The sample preparation procedure used for TEM analysis of the particles was as follows. The particles were first dispersed in ethanol 0.1 mg/mL suspension in a glass beaker and beaker was sonicated for 10 min. One drop of sample suspension was placed on a carbon-coated grid (Ted Pella, USA) and dried at room temperature overnight before analysis under TEM.

## 2.6 Particle size analysis with dynamic light scattering

Dynamic light scattering (DLS) was performed using a Photocor-FC light-scattering instrument employing a 5 mW laser light source at 633 nm and a logarithmic correlate instrument to determine the mean equivalent hydrodynamic diameters of the samples. For the analysis, a suspension of ~0.1 mg/mL concentration of silica sample was made in ethanol. The suspension was sonicated for 30 min prior to analysis. The instrument measures the change of intensity of the laser light with time at 90° angles after interaction with spherically shaped particles suspended in liquid media. The diffusion coefficient was determined from the correlation function, and, assuming the Stokes–Einstein equation is valid, the equivalent hydrodynamic diameter distribution was obtained using the Dyna-LS software package supplied by Photocor.

## 2.7 Dissolution of cisplatin from silica particles

Dissolution of cisplatin from the surface of silica particles was studied in phosphate-buffered saline (PBS) with pH 7.4, at room temperature (25 °C). In this study, ~30 mg of cisplatin-functionalized silica samples were suspended in 50 mL of PBS for 48 h in a conical flask. Ten milliliters of the sample was taken at the end of the specified time period (24, 36, and 48 h). Sample was centrifuged at 3,500 rpm for 15 min, and the supernatant was collected. Clear supernatant was analyzed for platinum using the inductively coupled plasma mass spectrometer. A 10-mL volume of fresh dissolution medium (PBS solution) was added to make up the volume after withdrawal of sample. The dissolution rate constant of the cisplatin from the silica surface at different time points (24, 36, and 48 h) was calculated using the modified Noyes and Whitney equation

(Wurster and Taylor 1965).

$$\frac{dC}{dt} = Ak(C_s - C)$$

where,  $dC/dt$ =rate of dissolution,  $A$ =surface area of the particle,  $C$ =concentration of the cisplatin in the PBS buffer at 25 °C,  $C_s$ =saturation concentration of the cisplatin in the PBS at 25 °C,  $k$ =dissolution rate constant, which is defined as  $k=D/h$ , where  $D$ =diffusion rate of cisplatin, and  $h$ =diffusion layer thickness.

## 2.8 Cell culture

The breast cancer cells (MCF-7) were maintained in Dulbecco's modified eagles medium (DMEM) supplemented with 2 mM L-glutamine and balanced salt solution adjusted to contain 1.5 g/L Na<sub>2</sub>CO<sub>3</sub>, 0.1 mM nonessential amino acids, 1 mM sodium pyruvate, 2 mM L-glutamine, 1.5 g/L glucose, 10 mM (4-(2-hydroxyethyl)-1-piperazineethane sulfonic acid), and 10 % fetal bovine serum (GIBCO, USA). Penicillin and streptomycin (100 IU/100 µg) were adjusted to 1 mL/L. The cells were maintained at 37 °C with 5 % CO<sub>2</sub> in a humidified CO<sub>2</sub> incubator.

## 2.9 Metabolic activity assay

The mitochondrial activity of MCF-7 cells was measured after treatment with the cisplatin-functionalized silica samples using the MTT assay. This test was performed on MCF-7 cells after 24, 36, and 48 h of incubation with the samples, as described by (Mosmann 1983). Cells were grown in a 24-well plate in DMEM media with 10 % fetal bovine serum at 37 °C and 5 % CO<sub>2</sub>. In this study, silica/cisplatin particles were added with the weight ranging from 13 to 144 µg/mL corresponding to the amount needed to give a concentration of surface attached cisplatin equal to 5 µg/mL in each well of a single 24-well plate. Four replicates were performed for each sample. Positive and negative controls were included on each plate. The MTT assays involved the following steps: the growth medium was removed from the culture wells and washed with 300 µL PBS once. After washing, 300 µL of MTT solution (0.5 mg/mL) was added in each well of the plate. For the reduction of tetrazolium salt, plates were

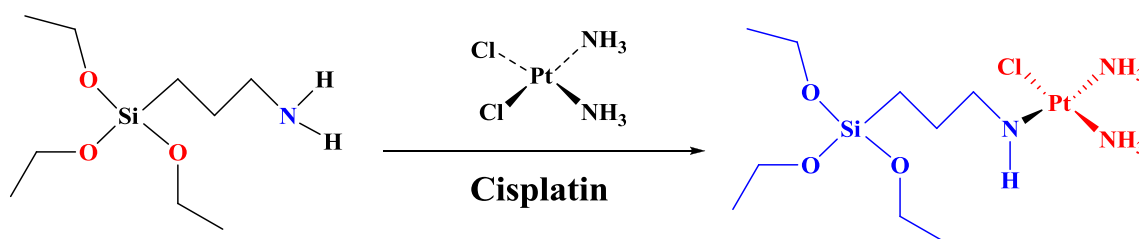
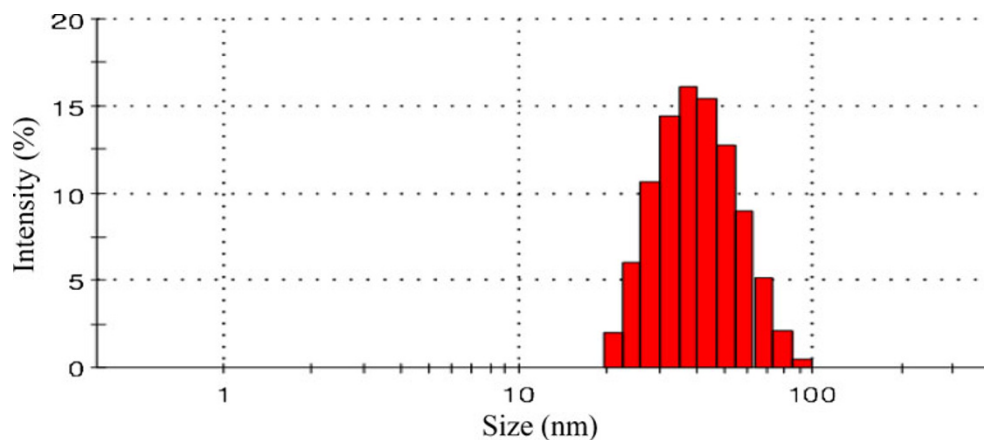


**Fig. 1** Scheme shows the synthesis of cisplatin-functionalized silica nanoparticles complex

**Fig. 2** Diameter measured by dynamic light scattering for cisplatin-functionalized silica nanoparticles



incubated at 37 °C for 2 h. The tetrazolium salt was reduced to a formazan (blue) product by the active mitochondria of the cells. In each well, 300  $\mu$ L of solubilizing buffer (10 % Triton X-100 with 0.1 N HCl in anhydrous isopropanol) was added to dissolve the reduced tetrazolium salt. The color of reduced salt was measured at 570 nm using microplate reader (SpectraMax M5, Molecular Devices, Sunnyvale, CA). The absorbance at 570 nm was taken as the index of mitochondrial activity.

### 2.10 Fluorescence microscopy

Cellular viability produced by the combination of cisplatin and silica particles was examined using fluorescence microscopy after staining the MCF-7 cell with the live/dead system (Molecular Probes, USA). After incubation with the samples in 96-well plates, cells were stained by adding DAPI and JC-1 to reach a final concentration in the well plates of 4  $\mu$ M DAPI and 2  $\mu$ M JC-1. DAPI undergoes fragment DNA conversion to fluorescent DAPI (blue, 340 nm wavelength), which is retained well within live cells. JC-1 enters cells with damaged membranes, and undergoes a fluorescence enhancement (brown, 635 nm wavelength) upon binding to DNA fragments. Cells were incubated with the dyes for 20 min in 100  $\mu$ L PBS, and imaged under the fluorescence microscope (Nikon instrument Inc., USA) using an excitation wavelength of 488 nm.

### 2.11 Cell sectioning for electron microscopy

Cisplatin-functionalized silica-treated MCF-7 cell line was grown on the 24-well cell culture plates. MCF-7 cells exposed to silica (Triton X-100) were used as the control. Cells were washed with PBS buffer and collected in centrifuge tubes after harvesting. Cells were washed with 0.13 M phosphate buffer three times for 10 min. At the end of the washing, cells were treated with a fixative solution (2 % glutaraldehyde) overnight at 4 °C. After fixation, cells were washed with 0.1 M phosphate

buffer three times for 10 min to remove the excess glutaraldehyde. Cells were post-fixed with 1 % OsO<sub>4</sub> in PBS for 60 min and washed with double-distilled water three times for 10 min. After washing, cells were dehydrated at room temperature in 30, 45, 65, 90, and 100 % ethanol for 10 min each. Cells were then infiltrated with propylene oxide and LR white resin mixture for 4 h. Cells were kept in fresh pure LR white resin overnight at room temperature. Finally, the cells were embedded in capsules

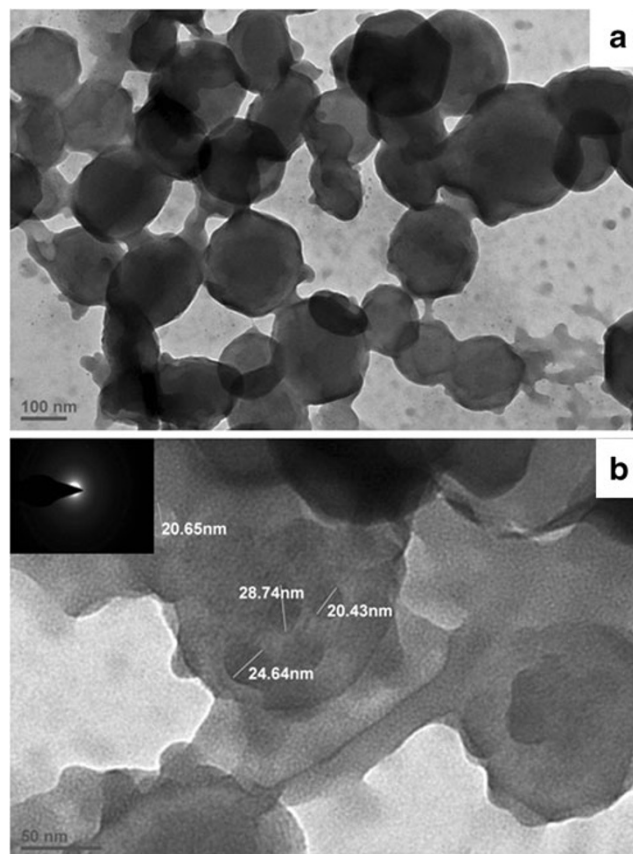


**Fig. 3** **a** Transmission electron microscope image of cisplatin-functionalized silica particles. **b** Selected area electron diffraction and higher magnification image

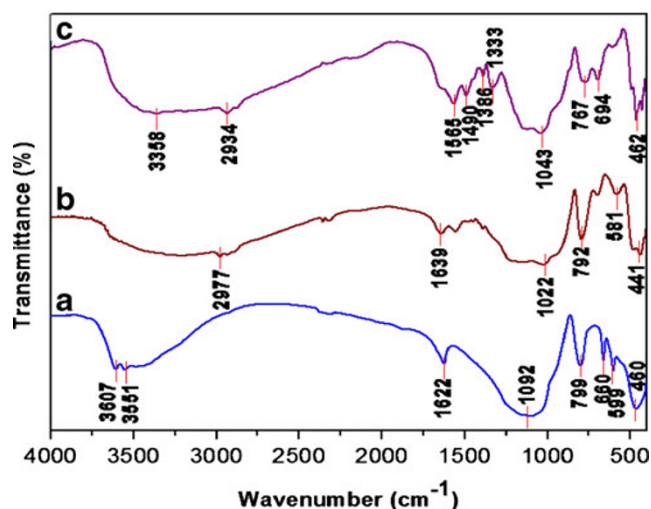


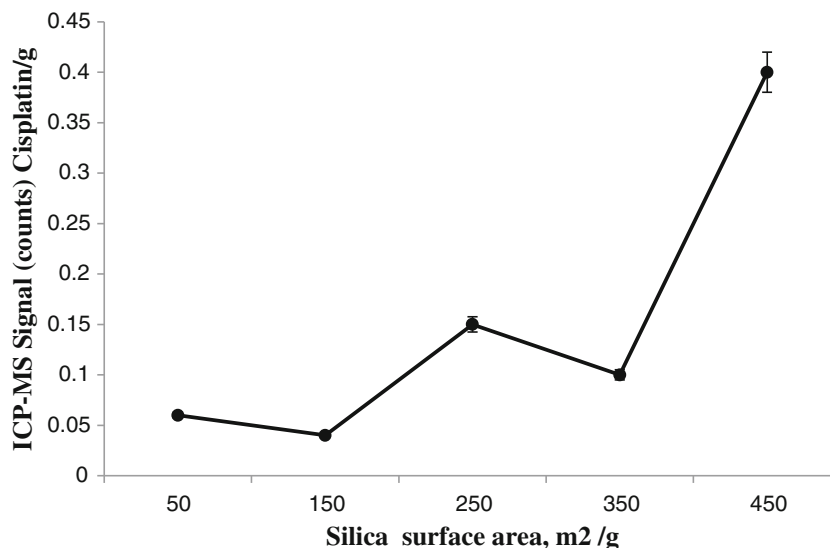
**Fig. 4** FT-IR spectra, before and after the reaction with cisplatin-functionalized silica nanoparticles. **a** Silica nanoparticles, **b** cisplatin, **c** cisplatin-functionalized silica nanoparticles

(Electron Microscopy Sciences, USA) with freshly prepared LR white resin. Polymerization was carried out in an oven at 60 °C for 24 h. Sections from the embedded cells were cut on an Ultra cut microtome (Reichert, Wien, Austria) and collected on 100-mesh copper TEM grids (Ted Pella Inc.). Ultrathin sections mounted on copper grids were stained with 1 % aqueous uranyl acetate (Ted Pella Inc.) for 15 min and lead citrate (Electron Microscopy Sciences, USA) for 1.5 min.

## 2.12 Statistical analysis

Appropriate statistical procedures (Student *t* test for means, Stat graphics plus 3.3 software) were applied in the statistical analysis of the experimental data.

**Fig. 5** Estimation of maximum and minimum cisplatin attachment to the silica surface and inductively coupled plasma mass spectrometry result. *Error bars* represent standard deviations of triplicate measurements



## 3 Results and discussion

### 3.1 Synthesis and characterization of cisplatin-functionalized silica particles

In this study, schematic diagrams shows (Fig. 1) the surface of silica particles was modified by the attachment of cisplatin molecules, making use of the silanol groups on the silica surface. Silanol groups are thought to be predominantly isolated from each other, with the surface concentration reported to vary between two and four silanol groups per square nanometer (Fripiat 1982; Iler 1979; Katz and Milewski 1987; Mathias and Wannemacher 1988). In a study of silica, the silanol surface concentration was found to vary only slightly with surface area: 2.1 groups/nm<sup>2</sup> for Triton X-100, which is made at high flame temperatures to facilitate larger primary particle diameters, versus 2.4–2.5 groups/nm<sup>2</sup> reported for Aerosil samples (Bhowmick et al. 2010). The observed reductions in the specific surface areas of the cisplatin-functionalized particles are explained by the attachment of cisplatin molecules on the particle surface. The mean equivalent hydrodynamic diameters of cisplatin-functionalized silica samples, as determined by DLS, are given in Fig. 2. Smaller particles, with respect to hydrodynamic diameter, have a greater surface area and are more easily dispersed in aqueous solutions, because of the presence of higher concentration, on a per gram of silica basis, of silanol groups on the surface of the higher specific surface area.

Silica particle morphology was observed using TEM. The TEM image of the cisplatin-functionalized silica sample in Fig. 3a shows particles that are round in shape, ranging from 20 to 90 nm in diameter. The electron diffraction pattern, given in Fig. 3b (inset), shows the amorphous nature of the sample. In Fig. 3b, spherically shaped dark spots, believed to

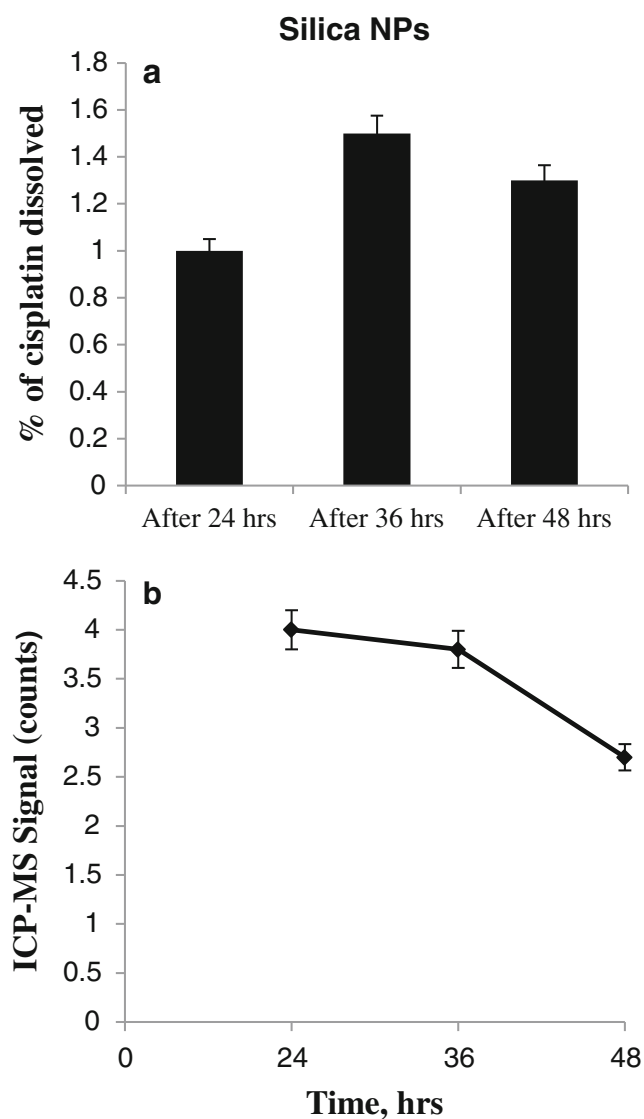


**Fig. 6** **a** Percentage cisplatin dissolved as a function of time. **b** Dissolution rate of cisplatin from the surface of silica particles to PBS buffer estimated by inductively coupled plasma-mass spectrometry. Error bars represent standard deviations of triplicate measurements

be platinum, are uniformly distributed on the surface of the particles. Mapping of the platinum also suggests a relatively uniform distribution of platinum on the silica particles. Oxygen and silicon result from the silica particles, and carbon from the TEM grid support and/or the APTES linker molecule on the particles.

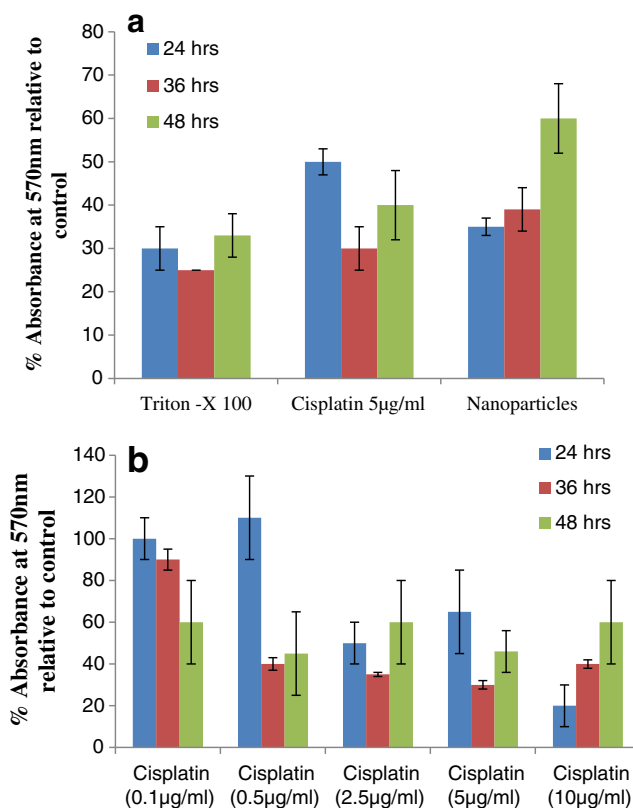
### 3.2 FT-IR characterization of cisplatin-functionalized silica nanoparticles

Figure 4a shows the FT-IR spectra of silica nanoparticles, the characteristic property of silica nanoparticles was showed by the N–H and O–H stretching vibration at  $3,607\text{ cm}^{-1}$  and the

$\text{SiH}_3\text{OH}$  bending vibration at  $1,622\text{ cm}^{-1}$ . The broad band spectrum at  $2,977$  and  $1,639\text{ cm}^{-1}$  shows the presence of cisplatin (Fig. 4b). The PEGs bending vibration at  $1,639\text{ cm}^{-1}$  demonstrating the characteristic property of cross-linked silica nanoparticles functionalized with cisplatin. The characteristic peak at  $1,565$  and  $1,386\text{ cm}^{-1}$  clearly reveals bending vibration of  $\text{SiH}_3\text{OH}$  and stretching vibration of PEGs, respectively. The characterized small peak at  $1,565$  and  $1,490\text{ cm}^{-1}$  shows the HCL removed stretching of cisplatin-functionalized silica nanoparticles (Fig. 4c). This result clearly shows the cross-linking of cisplatin-functionalized silica nanoparticles (supporting data S3).

### 3.3 Amount of cisplatin attached to the silica surface

ICP-MS results for the amount of cisplatin attached to the silica surface are presented in Fig. 5, along with estimates of the minimum and maximum expected cisplatin loading. The maximum amount of cisplatin attachment to the silica particles was estimated assuming that silica particles contain  $2.5$  silanol groups/ $\text{nm}^2$  on the surface (Katz and Milewski 1987), and assuming a 1:1 binding ratio between the silanol



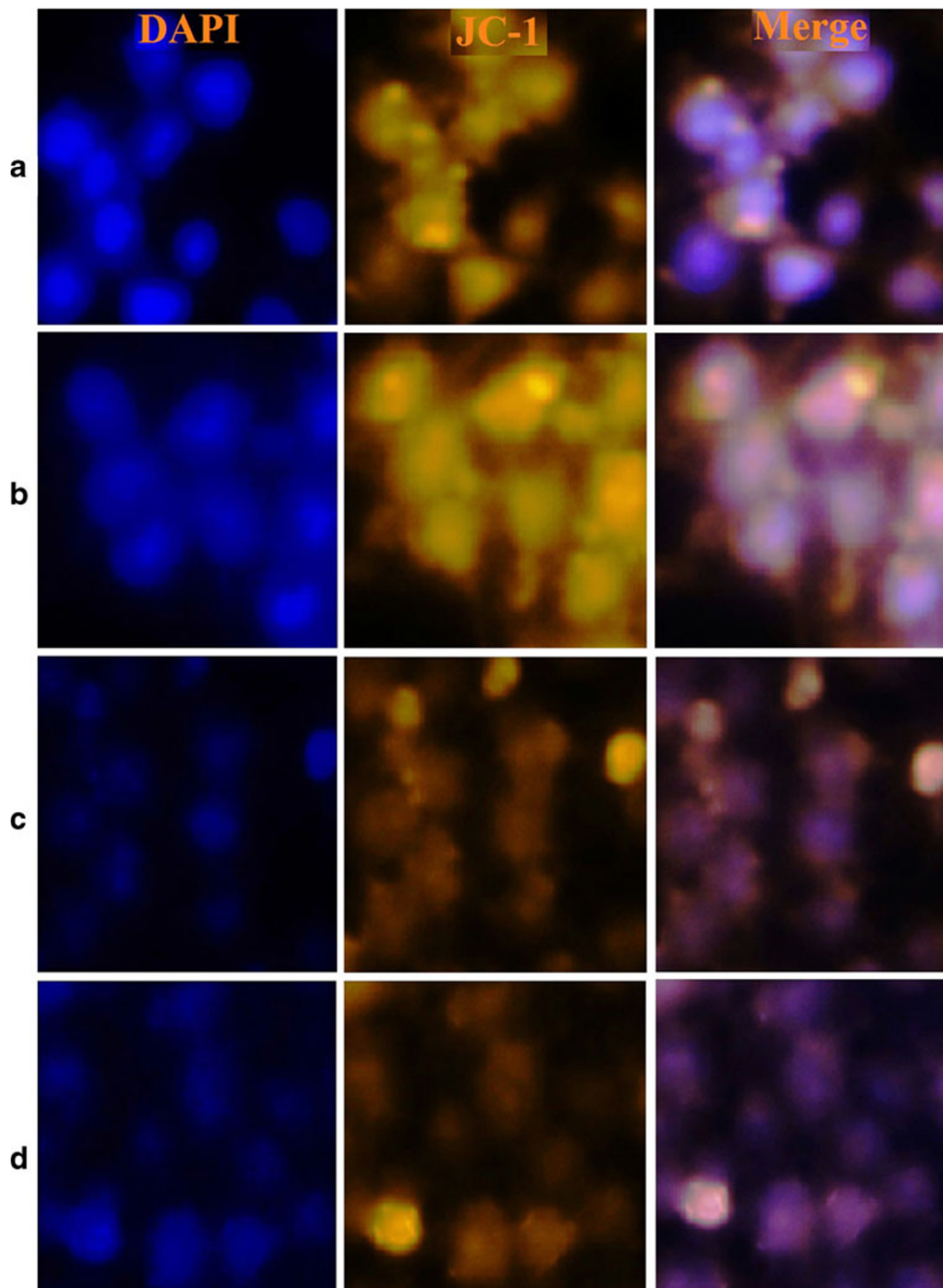
**Fig. 7** MTT assay of cisplatin-functionalized silica particles on MCF7. **a** After 24, 36, and 48 h and **b** dose-dependent study of free cisplatin. Results are presented as mean values compared to the control, and error bars represent standard deviation of four experiments. Asterisks denote statistically significant ( $p > 0.05$ ) differences between experiment and control

groups, APTES, and cisplatin. A minimum amount of cisplatin attachment was estimated assuming that 50 % reaction had occurred between the silanol groups and APTES, and between APTES and cisplatin. As shown in Fig. 5, the cisplatin loading is projected to be roughly proportional to the surface area of the silica nanoparticles. This was observed experimentally, with cisplatin loading ranging from maximum 0.4 g cisplatin/g silica for APTES to 0.039 g cisplatin/g silica for silanol groups. These results indicate the significance of nanoparticle-based materials in terms of their high loading capacity.

### 3.4 Dissolution of cisplatin from silica particles

Cisplatin-functionalized silica particles were used to investigate the release of cisplatin in PBS buffer (pH 7.4) with time. The percentages of cisplatin released from functionalized silica samples are shown in (Fig. 6a) and the dissolution rate constants of cisplatin from the samples are shown in Fig. 6b. The solubility of cisplatin in water is 2,350 mg/L (Kim et al. 2009). As shown in Fig. 6a, the percentages of cisplatin released are low but non-zero. In Fig. 6b, it can be seen that the dissolution rate constant of cisplatin from the cisplatin-

**Fig. 8** Live/dead images of MCF7 cells viewed under the fluorescence microscope after interaction with **a** control, **b** silica nanoparticles, **c** free cisplatin, **d** cisplatin-functionalized silica nanoparticles



functionalized silica particles is ten times greater than that of the lower specific surface area of surfactant (supporting data S1) 50 samples at 24 h. It can also be observed that the cisplatin dissolution rate decreases with time for all of the cisplatin-functionalized samples. Results also indicate that the dissolution of cisplatin in PBS buffer from the particle surfaces does not reach equilibrium within 48 h of time. This higher dissolution rate constant of cisplatin from the cisplatin-functionalized silica nanoparticles is attributed to the higher specific surface areas of the particles compared to the other samples (supporting data S2).

### 3.5 In vitro effects on metabolic function

We evaluated the effects of cisplatin-functionalized silica nanoparticles and cisplatin alone on cellular metabolic activity using the MTT assay after 24, 36, and 48 h, and the results are presented in Fig. 7a. MTT results for different doses of free cisplatin after 48 h are represented in Fig. 7b. Significant differences ( $p \leq 0.05$ ) between control and sample, as denoted by asterisks in Fig. 7a, were observed for the surface area samples, Triton X-100-cisplatin, at the earlier time points. Significant differences between control and sample were observed for silica-cisplatin samples by 48 h. The MCF-7 cells exhibits the smallest decrease in metabolic activity in the case of cisplatin-functionalized silica sample, even after 48 h of incubation. Student *t* test indicates that the MTT

results for each of the silica samples and the 5  $\mu\text{g}/\text{mL}$  cisplatin sample are significantly different ( $p \leq 0.05$ ). Results also show that reduction in metabolic activity after treatment with the Triton-cisplatin construct (45 % compared to control) is very close to the response from the cells treated with cisplatin (38 % compared to control). An almost equal reduction in metabolic activity can be observed after 48 h when the cells are incubated with free cisplatin at different doses (0.1–10  $\mu\text{g}/\text{mL}$ ) as shown in Fig. 7b. With the silica-cisplatin system, it is important to note, however, that no apparent synergistic effects were observed in terms of adverse effects on cellular function, unlike in prior reports of the benzo(a)pyrene/iron oxide micron-sized particle system (Garcon et al. 2001; Garry et al. 2004). Nor were any mitigative effects on cellular function observed, as in the case of silica synthesized with chitosan, compared to silica synthesized in the absence of chitosan (Chang et al. 2007). Exposure to the combination of cisplatin with silica that had the highest specific surface area resulted a similar effect on metabolic activity as compared to exposure to the equivalent amount of free cisplatin.

The MCF-7 cells were treated with cisplatin-functionalized silica particles of specific surface area for 24 h, and viability was observed by staining live and dead cells with DAPI and JC-1, respectively. Fluorescence stained breast cancer cells after treatment with the control (nontreated), Triton X-100 silica particles, cisplatin-functionalized particles, and free cisplatin are shown in

**Fig. 9** Transmission electron microscope images of MCF7 cells **a** after interaction with cisplatin-functionalized silica particles, *inset* shows extracellular particles, **b** the same sample suggesting endocytosis of the silica particles, *inset* shows particles at higher magnification, **c** and **d** control cells showing a smaller nucleus compared to the cisplatin-functionalized particle-treated cell

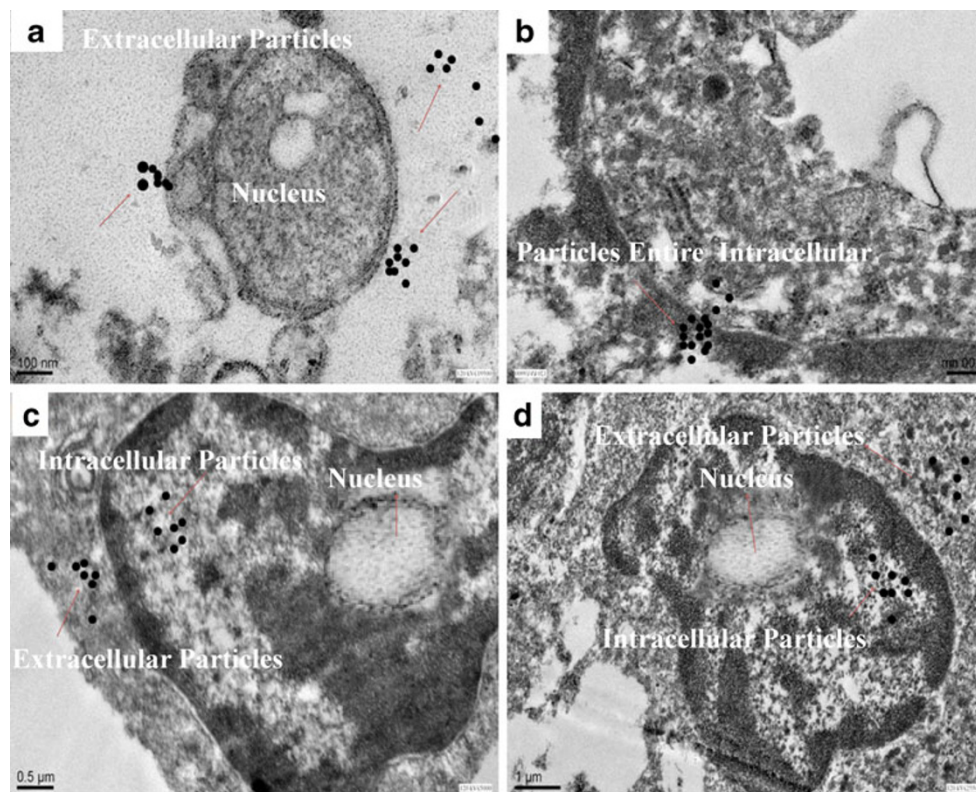


Fig. 8a, b, c, and d respectively. Remarkable morphological changes were observed under the fluorescence microscope when cells were treated with cisplatin-functionalized particles. In Fig. 8d, the number of cells remaining after treatment with the particles is less than the others. The MTT results also have shown that the greatest reduction in metabolic activity was produced by the treated cells, which is in agreement with the fluorescence microscopy images. Results showed that after 24 h of incubation, cisplatin-functionalized silica particles and free cisplatin have the strongest adverse effect on viability compared to the control. In the fluorescence images, most of the cells appeared dead after treatment with cisplatin-functionalized silica particles and free cisplatin, Fig. 8c, d. In contrast, treatment with control (nontreated) led to slate significant adverse effects in the cells; most of the cells are alive as shown in Fig. 8a. This study indicates that nanoparticle-mediated morphological alteration may occur in the cells and to study these morphological changes at a higher level of resolution, we further observed them in the transmission electron microscope.

### 3.6 Cellular response to cisplatin-functionalized silica particles

Cisplatin-functionalized silica particle breast cancer cell interactions were investigated by TEM analysis of thin sectioned cell samples. Representative micrographs are shown in Fig. 9, with images chosen after analyzing 50–100 cells from each sample. The morphology of MCF-7 cells after treatment with cisplatin-functionalized silica particles is shown in Fig. 9a, b whereas MCF-7 cells after treatment with control silica particles are shown in Fig. 9c, d. TEM images clearly show the internalization of the both control and cisplatin-functionalized silica particles inside the cells (Fig. 9c). In both the cases, extracellular particles are also visible in the images. Images also show that intracellular particles are confined in membrane-bound vacuoles (Fig. 9a). Internalized particles are found in aggregated form and may have entered the cells by the endocytosis process as suggested by the image in Fig. 9b. Membrane-bound aggregated particles are observed to be very close to the nucleus of the cell in some cases. The morphological changes in MCF-7 cells after 48 h of growth are also shown in Fig. 9. The images shown in Fig. 9 are the representatives of entire cell population after analyzing 50–100 cells in each sample. Images of cells after treatment with control silica particles (Fig. 9c, d) revealed that the cell membranes are more integrated compared to the cells treated with cisplatin-functionalized silica particles (Fig. 9a, b). It also can be observed that nucleus of the cells treated with cisplatin-functionalized silica (Fig. 9a) is much larger compared to the cells treated with control silica particles (Fig. 9c) (Meijer et al. 2001).

TEM analysis of the MCF-7 cells can shed light in understanding the possible interaction mechanisms of cisplatin-functionalized silica particles with the cells. Cisplatin must be able to react with DNA to affect cell function, so it needs to reach the cell nucleus. In the TEM images, both extracellular and intracellular particles are visible suggesting two possibilities. The extracellular particles may be releasing cisplatin into solution, which is then taken up by the cells. Free cisplatin is believed to enter cells via both passive and active transport routes (Ohmori et al. 1993). Cisplatin-functionalized silica nanoparticles can enhance both possible interaction mechanisms by bringing high loadings of cisplatin near the cells for passive transport of free cisplatin to take place. The intracellular particles, on the contrary, may carry bound cisplatin into the MCF-7 cells, which is then released into the cytoplasm with higher surface area corresponding to greater rates of active transport.

## 4 Conclusions

In conclusion, successful attachment of a controlled amount of toxic cisplatin molecules on the surface of the nano-sized silica particles was demonstrated and the particles were characterized in terms of particle size and surface area. In this study, we have demonstrated that the dissolution rate of cisplatin from the surface of the particles to the solution phase depends on the surface areas of the particles. Biological studies have shown that, the impaired cellular function in the MCF-7 induced by cisplatin-functionalized silica particles, as indicated by the reduced metabolic activity and cell viability. These effects appeared to be correlated with the cisplatin functionalized surface areas of the particles. Apparent uptake of the particles by the cells and morphological differences after active interaction with the cisplatin-functionalized silica particles were observed by TEM. The importance of our study lies in showing the combinatorial effect of relatively high surface area nanoparticles and toxic molecules at the cellular level. In the wake of increasing use of nanoparticles, which may be either surface modified prior to end use in drug delivery constructs or consumer products, or upon release into the environment, this study issues a cautionary note that the properties of the nanoparticles, especially specific surface area, may affect biological response.

**Acknowledgments** This work was financially supported by DST-NANOMISSION (DST No. SR/NM/NS-60/2010) Ministry of Science and technology and UGC-NON-SAP (G2/6966/UGC NON-SAP (Zoology)/2010) New Delhi, Govt. of India. The authors greatly acknowledged DRDO Centre for Life Sciences for nanoparticles characterization studies, Electron Microscopy Centre, AIIMS, New-Delhi and Sankara Nethralaya for their kind assistance with fluorescence microscopy studies. The authors are very much thankful to all faculty members

of the Department of Zoology, Bharathiar University for their constant support and encouragement throughout this study.

## References

- American Cancer Society (2012) Cancer facts and figures 2012. American Cancer Society, Atlanta
- Bhowmick TK, Yoon D, Patel M, Fisher J, Ehrman S (2010) In vitro effects of cisplatin-functionalized silica nanoparticles on chondrocytes. *J Nanoparticle Res* 12:2757–2770
- Bontha S, Kabanov AV, Bronich TK (2006) Polymer micelles with cross-linked ionic cores for delivery of anticancer drugs. *J Control Release* 114:163–174
- Chang JS, Chang KLB, Hwang DF, Kong ZL (2007) In vitro cytotoxicity of silica nanoparticles at high concentrations strongly depends on the metabolic activity type of the cell line. *Environ Sci Technol* 41:2064–2068
- Decatris MP, Sundar S, O'Byrne KJ (2004) Platinum-based chemotherapy in metastatic breast cancer: current status. *Cancer Treat Rev* 30:53–81
- Fripiat JJ (1982) Silanol groups and properties of silica surfaces. *ACS Symp Serc* 194:165–184
- Gan S, Yang P, Yang W (2009) Photo activation of alkyl C-H and silanization: a simple and general route to prepare high-density primary amines on inert polymer surfaces for protein immobilization. *Bio macromol* 10:1238–1243
- Garcen G, Gosset P, Garry S, Marez T, Hannotiaux MH, Shirali P (2001) Pulmonary induction of proinflammatory mediators following the rat exposure to benzo(a)pyrene-coated onto Fe<sub>2</sub>O<sub>3</sub> particles. *Toxicol Lett* 121:107–117
- Garry S, Nesslany F, Aliouat E, Haguenoer JM, Marzin D (2004) Hematite (Fe<sub>2</sub>O<sub>3</sub>) acts by oxydative stress and potentiates benzo[a]pyrene genotoxicity. *Mutat Res* 563:117–129
- Geng L, Osusky K, Konjeti S, Fu A, Hallahan D (2004) Radiation-guided drug delivery to tumor blood vessels results in improved tumor growth delay. *J Control Release* 99:369–381
- Giese B, McNaughton D (2003) Interaction of anticancer drug cisplatin with guanine: density functional theory and surface enhanced Raman spectroscopy study. *Biopolymers* 72:472–489
- Hill JM, Speer RJ (1982) Organo-platinum complexes as antitumor agents. *Anticancer Res* 2:173–186
- Iler RK (1979) The chemistry of silica: solubility, polymerization, colloid and surface properties, and biochemistry. Wiley, New York, xxiv, 866
- Jang LS, Liu HJ (2009) Fabrication of protein chips based on 3-aminopropyltriethoxysilane as a monolayer. *Biomed Microdevices* 11:331–338
- Junior AD, Mota LG, Nunan EA, Wainstein AJ, Wainstein AP, Leal AS, Cardoso VN, De Oliveira MC (2007) Tissue distribution evaluation of stealth pH-sensitive liposomal cisplatin versus free cisplatin in Ehrlich tumor-bearing mice. *Life Sci* 80:659–664
- Katz HS, Milewski JV (1987) Handbook of fillers for plastics. Van Nostrand Reinhold Co, New York
- Kim JK, Anderson J, Jun HW, Repka MA, Jo S (2009) Self-assembling peptide amphiphile-based nanofiber gel for bioresponsive cisplatin delivery. *Mol Pharm* 6:978–985
- Libertino S, Giannazzo F, Aiello V, Scandurra A, Sinatra F, Renis M, Fichera M (2008) XPS and AFM characterization of the enzyme glucose oxidase immobilized on SiO(2) surfaces. *Langmuir* 24:1965–1972
- Liu T, Wang S, Chen G (2009) Immobilization of trypsin on silica-coated fiberglass core in microchip for highly efficient proteolysis. *Talanta* 77:1767–1773
- Maeda H, Wu J, Sawa T, Matsumura Y, Hori K (2000) Tumor vascular permeability and the EPR effect in macromolecular therapeutics. A review. *J Control Release* 65:271–284
- Mathias J, Wannemacher G (1988) Basic characteristics and applications of Aerosil.30. The chemistry and physics of the Aerosil surface. *J Colloid Interface Sci* 125:61–68
- Meijer C, van Luyn MJA, Nienhuis EF, Blom N, Mulder NH, de Vries EGE (2001) Ultrastructural morphology and localisation of cisplatin-induced platinum–DNA adducts in a cisplatin-sensitive and -resistant human small cell lung cancer cell line using electron microscopy. *Biochem Pharmacol* 61:573–578
- Mosmann T (1983) Rapid colorimetric assay for cellular growth and survival: application to proliferation and cytotoxicity assays. *J Immunol Methods* 65:55–63
- Nguyen TH, Kim YU, Kim KJ, Choi SS (2009) Investigation of structural transition of dsDNA on various substrates studied by atomic force microscopy. *J Nanosci Nanotechnol* 9:2162–2168
- Ohmori T, Morikage T, Sugimoto Y, Fujiwara Y, Kasahara K, Nishio K, Ohta S, Sasaki Y, Takahashi T, Saijo N (1993) The mechanism of the difference in cellular uptake of platinum derivatives in non-small cell lung cancer cell line (PC-14) and its cisplatin-resistant subline (PC-14/ CDDP). *Jpn. J Cancer Res* 84:83–92
- Reedijk J (2003) New clues for platinum antitumor chemistry: kinetically controlled metal binding to DNA. *Proc Natl Acad Sci U S A* 100:3611–3616
- Rejeeth C, Kannan S, Muthuchelian K (2012a) Development of in vitro gene delivery system using ORMOSIL nanoparticle: analysis of p53 gene expression in cultured breast cancer cell (MCF-7). *Cancer Nano* 3:55–63
- Rejeeth C, Kannan S, Salem A (2012b) Novel luminescent silica nanoparticles (LSN): p53 gene delivery system in breast cancer in vitro and in vivo. *Journal of Pharmacy and Pharmacology* doi: 10.1111/j.2042-7158.2012.01547.x (In press)
- Rosenberg B (1977) Noble metal complexes in cancer chemotherapy. *Adv Exp Med Biol* 91:129–150
- Wang D, Lippard SJ (2005) Cellular processing of platinum anticancer drugs. *Nat Rev Drug Discov* 4:307–320
- Wurster DE, Taylor PW (1965) Dissolution rates. *J Pharm Sci* 54:169–175